PLOS ONE

RESEARCH ARTICLE

Seasonal variability in the persistence of dissolved environmental DNA (eDNA) in a marine system: The role of microbial nutrient limitation

Ian Salter[1,2]*

1 Sorbonne Universités, UPMC Univ Paris 06, CNRS, Laboratoire d'Océanographie Microbienne (LOMIC) Observatoire Océanologique, Banyuls/mer, France, **2** Faroe Marine Research Institute, Torshavn, Faroe Islands

* ian.salter@obs-banyuls.fr

Citation: Salter I (2018) Seasonal variability in the persistence of dissolved environmental DNA (eDNA) in a marine system: The role of microbial nutrient limitation. PLoS ONE 13(2): e0192409. https://doi.org/10.1371/journal.pone.0192409

Editor: Hideyuki Doi, University of Hyogo, JAPAN

Received: September 11, 2017

Accepted: January 22, 2018

Published: February 23, 2018

Data Availability Statement: All relevant data are within the paper and its Supporting Information files.

Funding: This work was carried out as part of the POPPYMED grant, awarded to Ian Salter, by the Institut National sciences de l'univers, Les Enveloppes Fluides et l'Environnement, Cycles biogéochimiques, environnement et ressources (INSU-LEFE-CYBER) (http://www.insu.cnrs.fr/lefe/presentation-cyber).

Competing interests: The author has declared that no competing interests exist.

Abstract

Environmental DNA (eDNA) can be defined as the DNA pool recovered from an environmental sample that includes both extracellular and intracellular DNA. There has been a significant increase in the number of recent studies that have demonstrated the possibility to detect macroorganisms using eDNA. Despite the enormous potential of eDNA to serve as a biomonitoring and conservation tool in aquatic systems, there remain some important limitations concerning its application. One significant factor is the variable persistence of eDNA over natural environmental gradients, which imposes a critical constraint on the temporal and spatial scales of species detection. In the present study, a radiotracer bioassay approach was used to quantify the kinetic parameters of dissolved eDNA (*d*-eDNA), a component of extracellular DNA, over an annual cycle in the coastal Northwest Mediterranean. Significant seasonal variability in the biological uptake and turnover of *d*-eDNA was observed, the latter ranging from several hours to over one month. Maximum uptake rates of *d*-eDNA occurred in summer during a period of intense phosphate limitation (turnover <5 hrs). Corresponding increases in bacterial production and uptake of adenosine triphosphate (ATP) demonstrated the microbial utilization of *d*-eDNA as an organic phosphorus substrate. Higher temperatures during summer may amplify this effect through a general enhancement of microbial metabolism. A partial least squares regression (PLSR) model was able to reproduce the seasonal cycle in *d*-eDNA persistence and explained 60% of the variance in the observations. Rapid phosphate turnover and low concentrations of bioavailable phosphate, both indicative of phosphate limitation, were the most important parameters in the model. Abiotic factors such as pH, salinity and oxygen exerted minimal influence. The present study demonstrates significant seasonal variability in the persistence of *d*-eDNA in a natural marine environment that can be linked to the metabolic response of microbial communities to nutrient limitation. Future studies should consider the effect of natural environmental gradients on the seasonal persistence of eDNA, which will be of particular relevance for time-series biomonitoring programs.

Introduction

The ability to measure species distribution is a fundamental requirement of biodiversity monitoring and conservation biology [1–3]. Environmental DNA (or eDNA) has recently emerged as a powerful tool to study patterns in biodiversity [4] and contribute to marine assessment programs [5,6]. Strictly eDNA can be defined as the total DNA recovered from a specific environment, in which sense it potentially covers intracellular DNA in organisms smaller than the sample, typically microorganisms [7,8], and extracellular or exogenous DNA in organisms larger than the sample [4,9]. Extracellular DNA may include dissolved components, including small mitochondrial organelles, or larger particulate cell fragments. High throughput sequencing of eDNA thus has the potential to describe spatial and temporal patterns in a wide range of organisms [10,11]. Following first successful application in water samples [2], eDNA species detection has been widely applied in aquatic settings: Previous studies have successfully demonstrated the detection of aquatic invertebrates [10,12], reptiles [13], amphibians [10,14], fish [15–20], marine mammals [20,21] and whale sharks [22].

The development of high-throughput sequencing and standardized procedures could facilitate metabarcoding of eDNA to be established in spatially [20] and temporally intensive monitoring of aquatic systems. However, before such approaches can be successfully implemented, an accurate understanding of the factors controlling the release and persistence of eDNA are required [23,24]. Previous studies have addressed eDNA degradation under experimental conditions by examining detection rates following the removal of target organisms. Successful detection of target organisms varies widely, ranging from 0.9–25 days [10,12,15,25,26], depending on the target organism and experimental set-up. Although these studies have highlighted the importance of considering eDNA degradation, it is difficult to extrapolate the findings to natural marine systems. A recent review paper provides a comprehensive discussion of the potential drivers of eDNA in aquatic systems [26]. A significant conclusion from this review is that no study has examined the effect of natural environmental gradients on eDNA degradation. This is particularly relevant considering that in the future eDNA may be applied to time-series biomonitoring of aquatic systems, where environmental gradients likely to influence eDNA degradation are known to vary seasonally.

The fate of DNA in aquatic systems has long been associated with microbial activity [27–35], largely through the action of membrane-bound and extracellular enzymatic activity [36–38]. Abiotic factors such as UV radiation, temperature and pH can directly impact denaturation of DNA [39–43] although together with salinity and dissolved oxygen concentrations [26] may exert an impact indirectly by modulating microbial metabolism and enzyme kinetics [44,45]. Based on the current literature it is reasonable to postulate that in marine systems the relationships between environmental variables and eDNA persistence is predominantly mediated through indirect effects on microbial physiology and enzyme activity. In this context the role of nutrient dynamics is probably of great significance. The microbial breakdown of dissolved organic phosphorous (DOP) pools is known to play a role in phosphorous nutrition under limiting conditions [35,46–48]. Nuclear magnetic resonance studies indicate that 75% of the DOP pool is represented by compounds containing P-ester bonds [49], which includes adenosine triphosphate (ATP) and DNA. To date the concentration of dissolved DNA has been shown to vary seasonally [31], spatially [32] and vertically [34] in the ocean and DNA uptake kinetics have been addressed in nutrient-enriched mesocosm experiments [35,50]. However, the seasonal dynamics of DNA uptake and turnover in response to nutrient limitation, or other environmental factors, remains largely unexplored.

The Mediterranean Sea is considered to be a marine biodiversity hotspot containing approximately 17,000 known species [51]. Shelf waters account for 20% of the sea, compared

to 7.6% globally [52]. The coastline is densely populated and expected to reach 175 million by 2025 (UN/MAP/BP/RAC 2005), rendering marine biodiversity particularly sensitive to anthropogenic threats [53] and subject to problems of invasive [54,55] and endangered [56–58] species. However, the absence of robust baselines in the Mediterranean has been identified as a major difficulty in evaluating marine health, thus compromising conservation efforts at the whole ecosystem level [59]. These defining features of the Mediterranean highlight it as a potentially strong beneficiary of recent advances in eDNA surveys. However, the Mediterranean is also a basin characterized by strong environmental gradients [51]. It is a low nutrient basin [60] characterized by west to east gradients in nutrient concentrations, N:P stoichiometry [61,62] and productivity gradients [63,64]. Inorganic phosphate concentrations in the Mediterranean are in the low nanomolar range [61,62] and limit primary productivity [65–67] and bacterioplankton [67–69]. In addition to these spatial gradients, time-series observations in the Northwest Mediterranean also exhibit seasonal gradients in temperature salinity, oxygen, pH, nutrients, phytoplankton biomass and bacterial activity [70–72], all of which are environmental factors thought to impact eDNA persistence [26].

The present work aims to address the paucity of observations in the degradation kinetics of dissolved eDNA (*d*-eDNA), as a component of extracellular DNA, across seasonally occurring environmental gradients in a marine system. Considering the great potential of eDNA to detect a wide range of aquatic organisms, and the possible contribution it can make towards marine policy issues, spatially and temporally intensive eDNA surveys are a likely prospect for the future. However, a better understanding of environmental controls on DNA turnover will be necessary to make the best possible use of future eDNA survey results in marine ecosystems. With these considerations in mind, the main objective of this study was to quantify the seasonal variability in *d*-eDNA turnover in relation to prevailing environmental conditions in the coastal Northwest Mediterranean. Particular emphasis was placed on the importance of nutrient limitation for driving microbial metabolism towards the utilization of *d*-eDNA as a phosphorous substrate.

Material and methods

Study site

Samples were collected from a fixed-point time-series site, SOLA, located in the Northwest Mediterranean at 42˚31′N, 03˚11′E. Station SOLA is a component of the French national coastal observation network SOMLIT (*Service d'Observation en Milieu LITtoral*). Sample collection and analytical procedures for the analysis of chlorophyll a, dissolved oxygen, pH, dissolved inorganic nutrients, temperature and salinity were carried out according to nationally standardized protocols and data quality procedures of SOMLIT, full details of which are archived at the URL: somlit.epoc.u-bordeaux1.fr. A brief description of these methods is provided below.

Sample collection

Surface seawater samples were collected bi-weekly from a depth of approximately 3 m. Sample water was collected into acid-washed (10% v/v HCl) polycarbonate carboys from 10 L Niskin bottles attached to a CTD rosette frame. Full depth profiles (25 m) of temperature, salinity and fluorescence were obtained in parallel from a Sea Bird SBE 19 profiler.

Chlorophyll. One litre of seawater was collected on a GF/F filter at low pressure (<0.2 bar). Samples were processed immediately after filtration or stored at -20˚C for a period < 1 week. Upon processing, samples were soaked in 90% acetone at 4˚C for a period of approximately

12–16 h and analyzed within 2 h. Fluorescence was measured before and after acidification to correct for phaeopigments [73,74].

Dissolved oxygen. Sampling bottles were washed with 1.2 M HCl, rinsed with deionized water, dried in an oven for 24 h and allowed to equilibrate to room temperature prior to sampling. According to SOMLIT protocols, dissolved oxygen is the first sample to be collected from a Niskin bottle immediately upon recovery. The bottles were rinsed twice with sample water and carefully filled using silicon tubing to avoid turbulence and bubbles. Dissolved oxygen was analyzed by titration following the Winkler method (1988) [74].

Dissolved inorganic nutrients. Nitrate, nitrite, phosphate and silicic acid were analyzed by colorimetry [75,76] on a flow-segmented analyzer (SEAL AA3; SEAL analytical). The analysis of unfiltered samples was conducted immediately or on samples stored at -20˚C for a maximum period of two months. Calibration was performed using high-purity certified standards (CERTPUR MERCK) of NO_3 (reference: 1.19811.0500), NO_2 (1.19899.0500), PO_4 (1.19898.0500) and $Si(OH)_4$ (1.12310.0500) prepared in a medium of ultra-pure artificial seawater. Detection limits were 0.05 μmol L^{-1} for NO_3+NO_2, 0.003 μmol L^{-1} for $Si(OH)_4$ and 0.006 μmol L^{-1} for PO_4.

Temperature and salinity. A Seabird SBE 19 sensor was used to acquire continuous measurements of conductivity, temperature and depth during CTD casts. The SBE 19 device is returned to Seabird annually for calibration. Minimum precision for the measurements was 0.01˚C for temperature and 0.01 units of salinity (or 0.05% of the measurement value). Raw CTD data were typically binned at 0.25 m depth intervals.

Bacterial production. The incorporation of ^{3}H-leucince was measured using the centrifugation method [77]. Subsamples (1.5 mL; three replicates and two blanks killed with 50% of trichloracetic acid (TCA)) were incubated for 2 h in the dark at *in situ* temperature with a mixture of ^{3}H-leucine (Perkin Elmer, (SA) 115.4 Ci $mmol^{-1}$) and non-radioactive leucine at final concentrations of 7 and 13 nM, respectively. Incubations were stopped by the addition of TCA to a final concentration of 5%. After a centrifugation step at 13,300 x g for 15 minutes the supernatant was discarded and 0.5 mL of 5% TCA were added. This step was performed twice with a second centrifugation for 5 minutes. Ethanol (0.5 mL of 70%) was added prior to the last centrifugation step of 5 minutes. The supernatant was discarded and 1 mL of PCS liquid scintillation cocktail was added. The radioactivity incorporated into bacterial cells was measured with a LS 6500 Beckman liquid scintillation counter.

Phosphate, ATP and DNA kinetics

The kinetics of orthophosphate, adenosine triphosphate (ATP), and deoxyribonucleic acid (DNA) uptake were measured by the Rigler bioassay approach [78] using a concentration series bioassay [35,79]. Phosphate and ATP bioassays were carried out using commercially available isotopes ($H_3{}^{33}PO_4$, AT-γ^{33}P) and radiolabeled DNA was synthesized as described below.

Radiolabelling of DNA. Radiolabelling of DNA follows the protocol of Løvdal et al. 2007. Random oligonucleotide primed synthesis was carried out using the Decalabel DNA labeling kit (Fermentas; K0621). This procedure results in products of variable lengths, here the average length was estimated to be 0.48 kbp according to an experimentally derived equation [80]. Lambda DNA HindIII digests (Fermentas; SM0101) were used as DNA templates and deoxyadenosine-[α-^{33}P]-triphosphate (3000 Ci $mmol^{-1}$ / 111 TBq $mmol^{-1}$; Perkin Elmer—NEG312H250UC) in 10 mL of tricine as the radioactive precursor. The half-life of phosphorous-33 is 25.4 days. A freshly-labeled DNA product was prepared at the beginning of each month throughout 2012 to ensure it was used within one half-life of ^{33}P and to avoid

significant shortening of the DNA chain length by radiochemical decay. Prior to use, primers and unincorporated deoxynuceotide triphosphates were removed through purification with a Genejet centrifugal filter device (Fermentas). The DE-81 filter-binding assay was used to determine typical label incorporation, DNA yield and specific activity of the purified product [81]. The radiolabelled DNA had label incorporation >98% with a specific activity ranging from 3.5×10^7–6.7×10^8 cpm μg^{-1}.

Bioassay incubations. Samples were collected in 1 L acid-washed thermos flasks [79] to maintain *in situ* temperatures until rate measurements could begin, which occurred within 30 minutes of sample collection. Carrier-free $^{33}PO_4^{-3}$ (as $H_3{}^{33}PO_4$; 155.8 Ci mg^{-1}, 5.76 TBq mg^{-1}, Perkin elmer—NEZ080) and gamma labeled ATP (Adenosine 5'-Triphosphate, [γ -33P]: 3000 Ci $mmol^{-1}$, 111 Tbq $mmol^{-1}$, Perkin Elmer—NEG302H) were diluted in ultra-pure water (0.2 μm sterile-filtered and autoclaved milli-Q) to create working solutions of 10.1 nM. The radiolabelled DNA product was diluted in ultra pure water to create a working solution of 10.1 ng mL^{-1}. For the standard addition bioassay experiments, 40 μL of each working solution was added to 4 mL of sample seawater in 5 mL sterile cryotubes to produce final tracer concentrations of 0.1 nM for $^{33}PO_4^{-3}$ and AT-$\gamma^{33}P$ and 0.1 ng mL^{-1} for DNA-^{33}P, corresponding to <10% of anticipated *in situ* concentrations [35]. For the phosphate and ATP incubations, samples were diluted with non-labeled standards to create a dilution series of 0, 4, 8, 12, 24, 48, 96, and 192 nM. A non-labeled DNA standard was created by diluting DNA III Hind stock in ultrapure water and was added to samples to create a dilution series of 0, 2, 4, 8, 12, 25, 50, 100 ng mL^{-1}. Samples were incubated at *in situ* temperatures in a temperature controlled incubation chamber.

All incubations were terminated after 15–60 minutes through the addition of 40 μL of a cold chase cocktail containing 100 mM of PO_4^{-3}, 100 mM of ATP and 50,000 μg L^{-1} of DNA resulting in final incubation concentrations of 1 mM PO_4^{-3} and ATP and 500 μg L^{-1} of DNA. Cold chase saturation [82] was favored over PFA fixation [79] to reduce the loss of incorporated tracer upon fixation. Blank incubations were performed identical to samples with the exception that the cold chase cocktail was added 15 minutes prior to the radioactive tracers. Upon completion of the incubation, blanks and samples were gently filtered (< 100 mbar vacuum) onto 25 mm 0.2 μm polycarbonate membranes (Millipore) backed with GF/C filters (Whatman). Prior to use, all membrane and glass fibre filters were soaked overnight in a 10 mM phosphate solution to minimize binding of unincorporated radioactive tracers during filtration. Membrane filters from $^{33}PO_4^{-3}$ and ATP incubations were rinsed with 3 mL of <0.2 μm-filtered sample water. DNA-^{33}P filters were rinsed with 3 mL of <0.2 μm-filtered sample water amended with low molecular weight salmon sperm (Sigma Aldrich) at a concentration of 10 μg mL^{-1}. After filtration polycarbonate membrane filters were transferred to 6 mL pony vials and 4 mL of Ultima Gold MV scintillation cocktail was added. Radioactivity on the filters was measured as counts per minute (cpm) with a LS 6500 Beckman liquid scintillation counter. Turnover was calculated according to Eqs 1 and 2

$$T_0 = t/(-\ln(1 - R)) \quad (1)$$

$$R = (S_{cpm} - B_{cpm}) - T_{cpm} \quad (2)$$

Where T_0 is the substrate turnover (h), t is the incubation time (h), ln is the natural logarithm and S_{cpm}, B_{cpm} and T_{cpm} are the radioactive counts of the samples, experimental blanks and tracer additions, respectively. Turnover was plotted against the concentration of non-labeled substrate additions (S*a*) to produce a linear representation (Lineweaver-Burk) of Michaelis-Menten substrate kinetics (Fig 1B and 1C). The y-intercept on the Lineweaver-Burk plot was

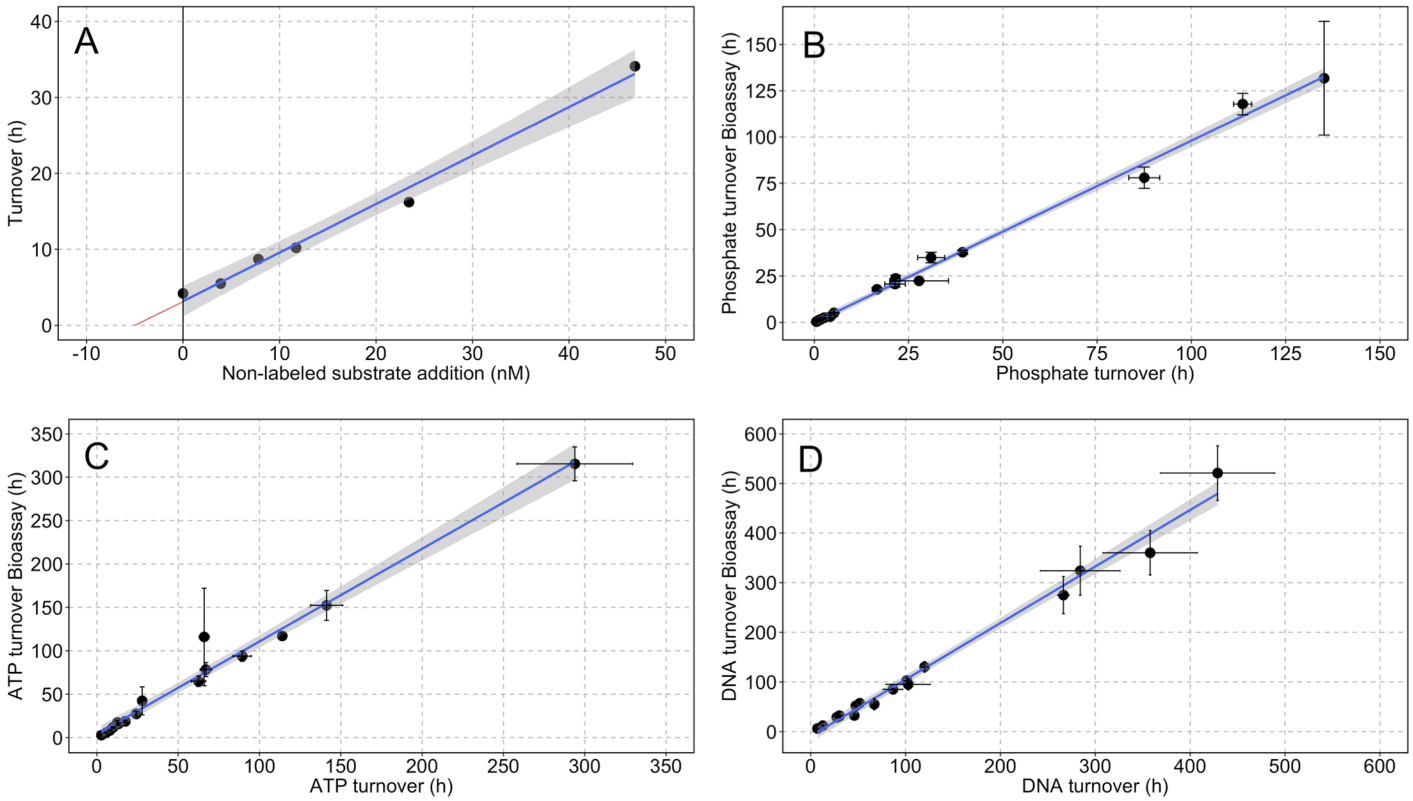

Fig 1. Radioactive bioassay concentration series. Panel (A) provides an example of the Rigler bioassay approach [78] using $^{33}PO_4^{3-}$ uptake data from 04.04.2012. The turnover of $^{33}PO_4^{3-}$ (T_0) was measured over a concentration series of non-labeled substrate additions (S*a*). The Lineweaver-Burk plot showed here is a linear representation of Michaelis-Menten uptake kinetics, whereby the slope of the regression ($1/V_{max}$) provides an estimate of substrate uptake rate, the negative intercept on the x-axis (k + S*n*: red line) is an estimate of the natural substrate concentration (S*n*) at ambient conditions (S*a* = 0), where k is the transport constant and assumed to be negligibly small [79], and the y-intercept is substrate turnover (k + Sn / V_{max}) at zero added substrate (S*a* = 0). In the case of phosphate, k + S*n* is taken as an estimate of biologically available phosphate and distinct from soluble reactive phosphorous (SRP) determined analytically. Panels (B-D) provide verification of the substrate uptake models by comparing (k + Sn / V_{max}) with turnover rates (T_0) measured from independent experiments. Error bars on measured turnover rates (x-axis) represent ± 1 σ from n = 3 replicates and error bars on bioassay estimates (y-axis) are estimated from the LINEST function of the concentration series (n>4). Regression statistics (slope ± standard error; p-value; r^2; F-statistic; degrees of freedom, p-value) for $^{33}PO_4^{3-}$ (1.01 ± 0.02; <0.001; 1.00; 2561; <0.001), AT^{33}P (0.96 ± 0.01; <0.001; 1.00, 1.08 x 10^4; 16, <0.001) DNA-^{33}P (1.02 ± 0.04; <0.001; 0.98. 671.3; 16; 0.001).

https://doi.org/10.1371/journal.pone.0192409.g001

used to calculate substrate turnover at ambient concentration (S*n*) (Fig 1A). Triplicate turnover measurements with no added substrate (S*a* = 0) were performed as an independent verification of the kinetic model and to validate the assumption that the transport constant (k) is negligibly small compared to ambient substrate concentrations [79]. The LINEST statistical function was used to determine standard errors on substrate uptake rates (V_{max}), ambient substrate concentrations (k + S*n*) and turnover at ambient concentrations ((k + S*n*) / V_{max}).

Partial least squares regression (PLSR) model

A statistical model to predict turnover of *d*-eDNA was developed based on projection to latent structures using PLSR. PLSR was selected as a predictive tool as it negates the assumptions of zero co-linearity in explanatory variables that characterize linear regression models, which is typically significant in environmental datasets [72]. PLSR linearly extracts a few latent variables that are most useful in modeling the response. The model was used to predict a single y–value (measured turnover of *d*-eDNA) from a set of environmental parameters (temperature, salinity, day length, pH, dissolved oxygen, dissolved inorganic nitrate + nitrite, biologically

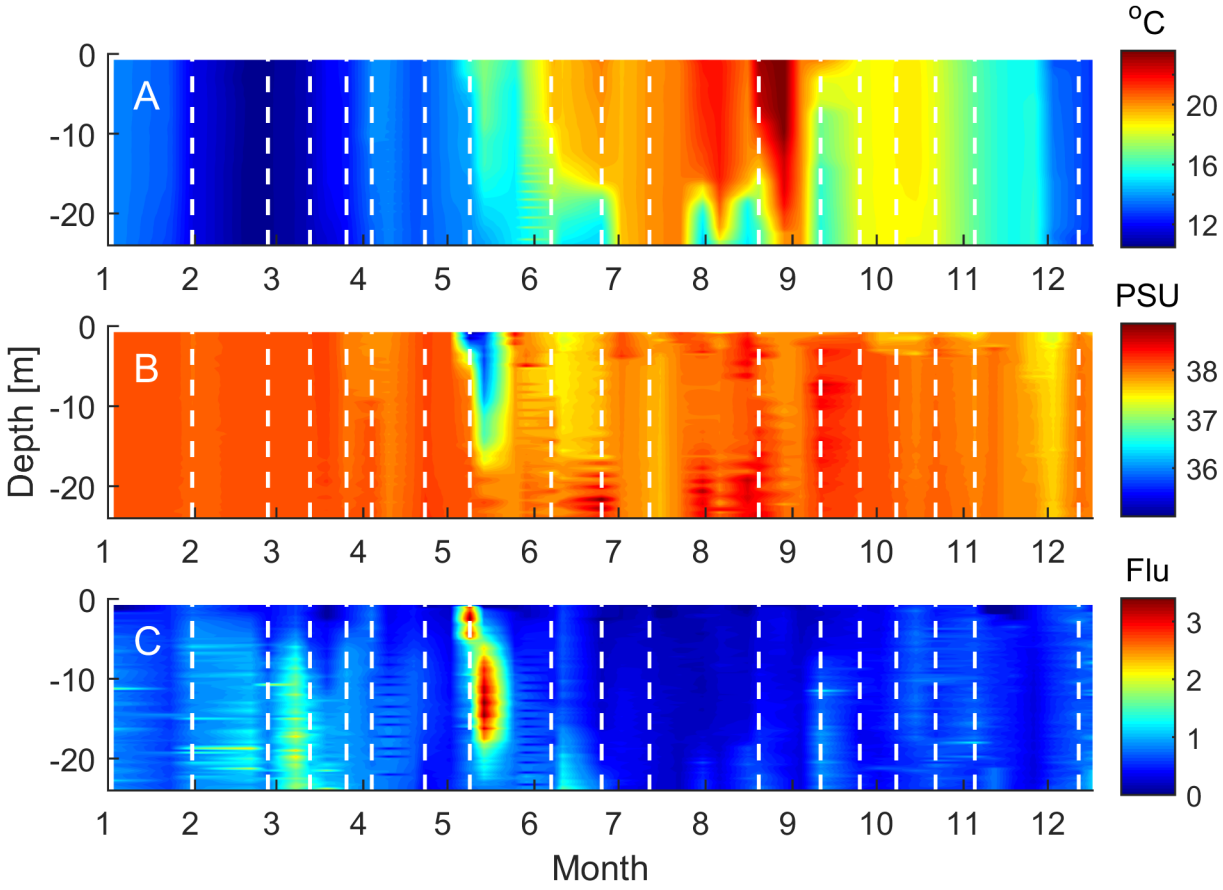

Fig 2. Depth profiles of environmental conditions. Full depth profiles of (A) temperature, (B) salinity and (C) fluorescence were measured at station SOLA in 2012. White dashed lines mark the dates when discrete samples were taken from the surface (3 m) to carry out phosphorous bioassay experiments (Solid black squares in Figs 3 and 4).

https://doi.org/10.1371/journal.pone.0192409.g002

available phosphorous, and phosphate turnover). The model was constructed using the seasonal dataset of approximately bi-weekly resolution. Input data were scaled to standardized values (mean = 0, variance = 1). The number of PLSR components was chosen by examining minima in root mean squared error of prediction (RMSEP) values following k-fold cross validation (k = 10) and cross-validated r^2 values, the latter taken as a measure of the PLSR model's goodness of fit [83]. The PLSR model was optimized with an r^2 value of 0.60 using two components (S1 File). Standardized regression coefficients were calculated for each predictor variable to ascertain the most important measured environmental parameters explaining the variance in microbially-mediated *d*-eDNA turnover. All analyses were performed in the R packages PLS and plsdepot [84] and the code is archived in the supporting information (S2 File).

Results

Environmental conditions

Full depth profiles of temperature, salinity and fluorescence were obtained with weekly resolution from CTD casts (Fig 2). The minimum temperature observed at 3 m from the CTD data was 10.6˚C on 27.02.2012 rising progressively to a maximum of 23.7˚C on 29.08.2012 (Fig 2A). Discrete samples for incubation work were collected on the 27.02.2012 and 20.08.2012, corresponding to the maximum seasonal temperature range of 12.2˚C (Fig 3A). Surface

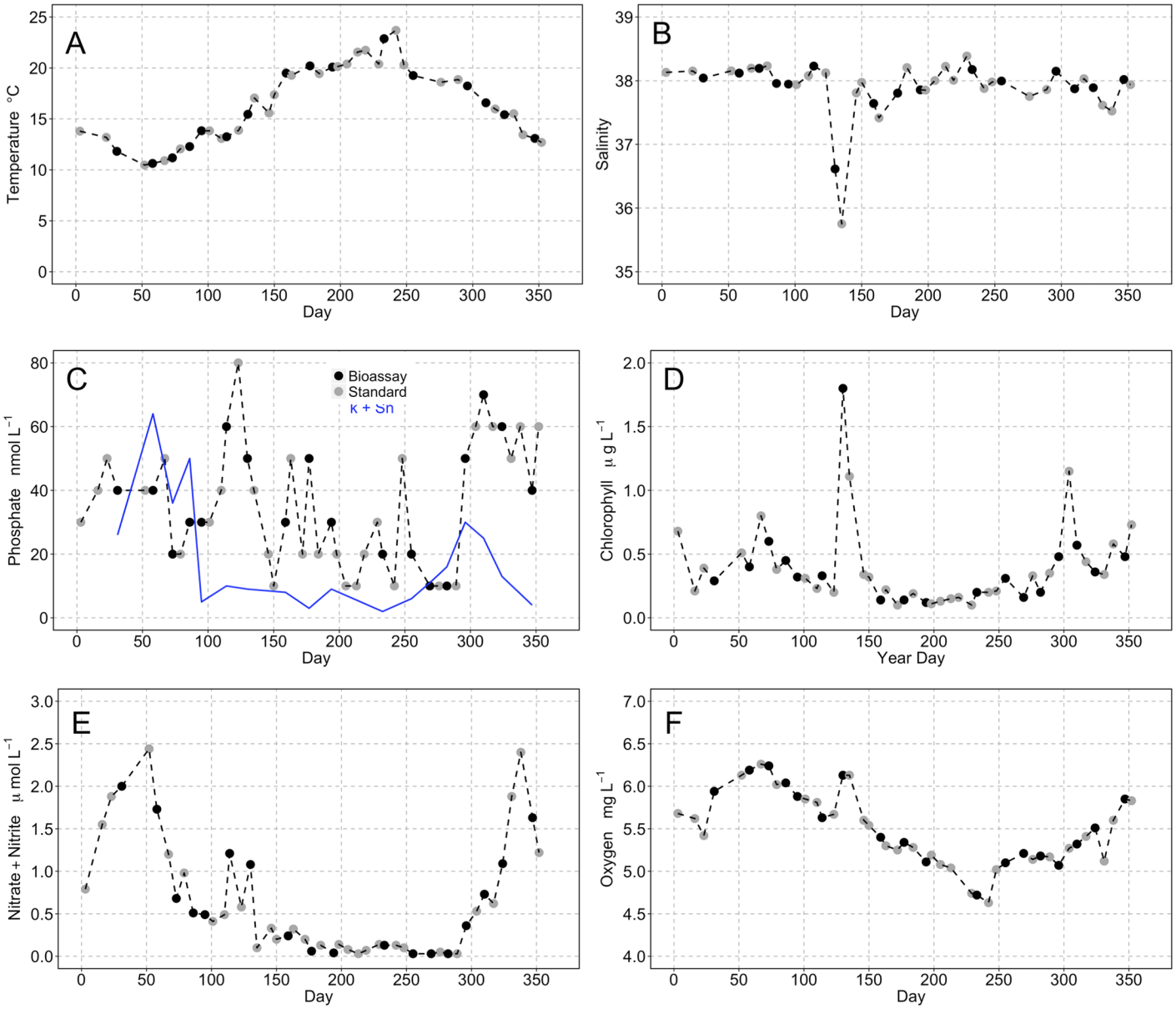

Fig 3. Time series observations of environmental parameters. Time series data of environmental parameters monitored in parallel to bioassay experiments during 2012 for (A) temperature, (B) salinity, (C) inorganic phosphate (PO_4^{3-}), (D) chlorophyll, (E) dissolved inorganic nitrogen (DIN = NO_3^{2-} + NO_2^-) and (F) dissolved oxygen. In panel (C) the dashed line is soluble reactive phosphorous (SRP) determined analytically and the solid blue line is an estimate of biologically available phosphate ($k + Sn$). Grey symbols mark the sampling dates when standard environmental parameters were measured and black symbols mark those where the kinetic bioassay experiments were conducted.

https://doi.org/10.1371/journal.pone.0192409.g003

salinity values were relatively constant throughout the year, fluctuating from 37.4 to 38.4 PSU with no clear seasonality. An episodic reduction in salinity occurred between the 9th and 14th May with surface values dropping to 35.7 PSU (Fig 3B). This low salinity feature penetrated to a depth of approximately 15 m in the water column (Fig 2B) and corresponded to significantly enhanced water column fluorescence values (Fig 2C). Surface chlorophyll values peaked at 1.8 µg L^{-1} on the 9th May in association with this low salinity feature (Fig 3D). Aside from these exceptionally high values, surface chlorophyll peaked at 0.8 µg L^{-1} on the 7th March and 1.15 µg L^{-1} on 30th October and were <0.2 µg L^{-1} for a 90 day period from 07.06—04.09.2012.

Table 1. Summary of sampling dates and inorganic phosphate (PO_4^{3-}) kinetic parameters estimated from the Rigler bioassay approach. The r^2 values are based on the regression statistics of substrate turnover against the concentration series of non-labeled substrate additions.

Sampling Date	V_{max} (nmol L^{-1} h^{-1})	$k + Sn$ (nmol L^{-1})	$(k + Sn) / V_{max}$ (h)	T_0 (h)	r^2
31/01/12	0.22 ± 0.02	26.1 ± 2.81	117.8 ± 5.82	113.6 ± 2.41	0.98
27/02/12	0.82 ± 0.09	63.6 ± 8.38	78.0 ± 5.76	87.5 ± 4.11	0.93
13/03/12	1.52 ± 0.17	35.9 ± 4.66	23.7 ± 1.64	21.6 ± 1.16	0.96
26/03/12	2.22 ± 0.24	49.7 ± 5.49	22.4 ± 0.42	22.8 ± 7.79	0.98
04/04/12	1.56 ± 0.08	4.96 ± 1.17	3.17 ± 0.73	4.21 ± 0.12	0.99
23/04/12	0.50 ± 0.08	10.4 ± 1.86	20.7 ± 1.63	21.4 ± 2.73	0.97
09/05/12	n.d.	n.d.	n.d.	1.25 ± 0.04	n.d.
07/06/12	8.49 ± 0.28	8.40 ± 0.51	0.99 ± 0.05	0.97 ± 0.05	0.99
25/06/12	6.50 ± 0.20	2.77 ± 0.41	0.43 ± 0.06	0.53 ± 0.03	0.99
12/07/12	3.60 ± 0.05	9.19 ± 0.28	2.55 ± 0.07	2.64 ± 0.09	0.99
20/08/12	3.57 ± 0.12	2.22 ± 0.24	0.62 ± 0.06	0.74 ± 0.01	0.99
11/09/12	3.46 ± 0.07	5.68 ± 0.18	1.64 ± 0.04	1.66 ± 0.03	1.00
25/09/12	2.07 ± 0.05	10.7 ± 0.63	5.14 ± 0.28	5.21 ± 0.09	1.00
08/10/12	0.90 ± 0.03	16.1 ± 0.89	17.8 ± 0.83	16.6 ± 0.44	0.99
22/10/12	0.79 ± 0.05	30.1 ± 2.19	37.8 ± 1.09	39.3 ± 0.63	0.97
05/11/12	0.72 ± 0.09	25.3 ± 3.73	35.0 ± 2.83	31.0 ± 3.58	0.96
19/11/12	0.14 ± 0.03	13.3 ± 4.39	92.0 ± 24.6	n.d.	0.96
12/12/12	0.03 ± 0.002	4.32 ± 1.05	131.7 ± 30.7	131.7 ± n.d.	0.99

https://doi.org/10.1371/journal.pone.0192409.t001

Values of soluble reactive phosphorous (SRP) fluctuated between 0.03 and 0.06 μM for most of the year with summer values frequently at, or close to the detection limit of 0.01 μM (Fig 3C). Bioavailable phosphorous concentrations ($k + Sn$), calculated from bioassay incubations, exhibited a more pronounced seasonality. Concentrations were between 0.03 and 0.06 μM from January through to March and then fell sharply and remained <0.01 μM until the end of September. Bioavailable phosphorous concentrations exhibited a secondary peak of 0.03 μM on 26.10.2012. Dissolved inorganic nitrogen concentrations (DIN) showed similar seasonality to bioavailable phosphorous (Fig 3E). Peak values of 2.5 μM were measured in early spring (21.02.2012) and early winter (03.12.2012), with significant depletion (<0.3 μM) observed between the 25th May and 15th October. Dissolved oxygen concentrations displayed a clear seasonal pattern with highest values >5.5 mg L^{-1} recorded in spring and lowest values (<5 mg L^{-1}) during summer (Fig 3F). Peak values of 6.13 mg L^{-1} were observed on the 9th and 14th May and associated to the episodic reduction in salinity (Figs 2B and 3B).

Isotope dilution experiments

The kinetic parameters and associated statistics calculated from the radioactive substrate bioassays are summarized in Tables 1–3. The substrate uptake data was well described by a linear representation of Michealis-Menten kinetics with r^2 values of 0.93–1.00, 0.85–1.00, and 0.77–0.99 for PO_4^{-3}, ATP and DNA, respectively (Tables 1–3). An independent assessment of turnover time (T_0) with no added substrate ($Sa = 0$) was positively correlated to turnover at natural substrate concentrations (Sn) estimated from the linear model ($k + Sn / V_{max}$) for PO_4^{-3} ($r^2 = 0.98$; Fig 1B), ATP ($r^2 = 0.99$; Fig 1C) and DNA ($r^2 = 0.98$; Fig 1D) and approximated a 1:1 relationship; slopes = 1.01 ± 0.02 (PO_4^{-3}), 0.96 ± 0.01 (ATP) and 1.02 ± 0.04 (DNA) (Fig 1).

The turnover of PO_4^{-3} showed a strong seasonal pattern with values steadily decreasing from 118 h in January to 1.2 h in May (Fig 4A). The turnover of phosphate remained < 6 h for

Table 2. Summary of sampling dates and ATP kinetic parameters estimated from the Rigler bioassay approach. The r^2 values are based on the regression statistics of substrate turnover against the concentration series of non-labeled substrate additions.

Sampling Date	V_{max} (nmol L^{-1} h^{-1})	$k + Sn$ (nmol L^{-1})	$(k + Sn) / V_{max}$ (h)	T_0 (h)	r^2
31/01/12	0.02 ± 0.003	2.24 ± 1.13	116.0 ± 56.1	66.0 ± 3.15	0.95
27/02/12	0.10 ± 0.01	4.21 ± 1.67	42.4 ± 16.1	27.9 ± 2.07	0.97
13/03/12	0.22 ± 0.03	17.5 ± 3.08	78.4 ± 8.04	67.1 ± 3.57	0.91
26/03/12	0.25 ± 0.05	16.3 ± 3.66	64.9 ± 6.07	62.5 ± 4.46	0.92
04/04/12	1.70 ± 0.03	19.9 ± 2.29	11.7 ± 1.02	9.90 ± 0.46	0.98
23/04/12	0.08 ± 0.03	12.3 ± 2.76	152.3 ± 17.2	141.2 ± 9.89	0.93
09/05/12	n.d.	n.d.	n.d.	2.80 ± 0.26	n.d.
07/06/12	0.95 ± 0.16	11.2 ± 2.04	11.8 ± 0.68	9.98 ± 1.14	0.89
25/06/12	1.01 ± 0.17	8.32 ± 1.43	8.25 ± 0.34	8.08 ± 0.07	0.92
12/07/12	0.32 ± 0.08	5.10 ± 1.28	15.83 ± 1.49	13.2 ± 0.16	0.85
20/08/12	0.94 ± 0.07	5.23 ± 0.46	5.58 ± 0.29	5.67 ± 0.06	0.97
11/09/12	0.48 ± 0.04	8.33 ± 1.23	17.5 ± 2.20	12.7 ± 0.30	0.97
25/09/12	0.04 ± 0.004	1.10 ± 0.15	27.3 ± 2.71	24.3 ± 0.31	0.98
08/10/12	0.03 ± 0.002	2.39 ± 0.23	93.9 ± 5.92	89.4 ± 5.60	0.98
22/10/12	0.01 ± 0.003	1.83 ± 0.14	18.8 ± 1.27	17.5 ± 0.40	1.00
05/11/12	0.04 ± 0.002	4.30 ± 0.29	117.1 ± 3.40	114.0 ± 1.44	0.99
19/11/12	0.01 ± 0.002	3.07 ± 0.54	315.4 ± 19.6	293.9 ± 35.6	0.94
12/12/12	0.03 ± 0.003	42.5 ± 3.78	1264.3 ± 34.3	1218.2 ± 339.3	0.97

https://doi.org/10.1371/journal.pone.0192409.t002

a five month period during summer, starting to rise again on the 8th October and reaching a maximum winter value of 131 h on 12th December. The turnover of DNA (Fig 4E) exhibited similar seasonality with an extended period of high turnover, ranging from 6–85 h, occurring between 9th May and 7th September. The pattern was comparable for ATP with turnover times

Table 3. Summary of sampling dates and DNA kinetic parameters estimated from the Rigler bioassay approach. The r^2 values are based on the regression statistics of substrate turnover against the concentration series of non-labeled substrate additions.

Sampling Date	V_{max} (nmol L^{-1} h^{-1})	$K + Sn$ (nmol L^{-1})	$(k + Sn) / V_{max}$ (h)	T_0 (h)	r^2
31/01/12	0.028 ± 0.007	14.6 ± 3.89	521.0 ± 55.2	428.9 ± 60.2	0.85
27/02/12	0.090 ± 0.01	4.95 ± 1.10	55.4 ± 11.3	67.0 ± 2.62	0.97
13/03/12	0.060 ± 0.009	5.37 ± 1.10	95.3 ± 11.1	102.8 ± 23.3	0.95
26/03/12	0.18 ± 0.008	9.12 ± 0.66	57.3 ± 3.1	51.6 ± 1.47	0.99
04/04/12	0.09 ± 0.007	8.87 ± 0.82	103.0 ± 5.46	101.2 ± 3.07	0.98
23/04/12	0.03 ± 0.008	9.28 ± 3.14	360.3 ± 44.8	357.8 ± 49.8	0.83
09/05/12	4.47 ± 0.46	28.8 ± 3.15	6.43 ± 0.25	7.03 ± 0.12	0.96
07/06/12	0.25 ± 0.01	7.19 ± 0.48	28.9 ± 1.39	27.5 ± 1.75	0.99
25/06/12	0.22 ± 0.03	7.28 ± 1.30	32.6 ± 4.37	45.9 ± 0.73	0.94
12/07/12	0.53 ± 0.09	16.3 ± 3.21	30.9 ± 2.78	30.1 ± 1.99	0.86
20/08/12	0.81 ± 0.12	9.93 ± 1.62	12.2 ± 0.75	12.7 ± 0.45	0.77
11/09/12	0.08 ± 0.002	6.60 ± 0.21	85.2 ± 2.23	86.8 ± 10.4	0.99
25/09/12	0.01 ± 0.001	3.02 ± 0.51	275.1 ± 37.3	266.4 ± 6.14	0.96
08/10/12	0.01 ± 0.001	3.68 ± 0.64	324.1 ± 49.3	284.1 ± 42.1	0.98
22/10/12	0.31 ± 0.02	16.3 ± 1.18	51.9 ± 2.67	47.5 ± 2.37	0.98
05/11/12	0.09 ± 0.01	12.1 ± 1.63	130.5 ± 10.7	120.0 ± 3.79	0.95
19/11/12	0.46 ± 0.07	14.8 ± 2.51	32.3 ± 2.09	30.3 ± 2.64	0.91
12/12/12	0.001 ± 0.0001	0.90 ± 0.27	794.4 ± 224.2	889.4 ± 20.4	0.99

https://doi.org/10.1371/journal.pone.0192409.t003

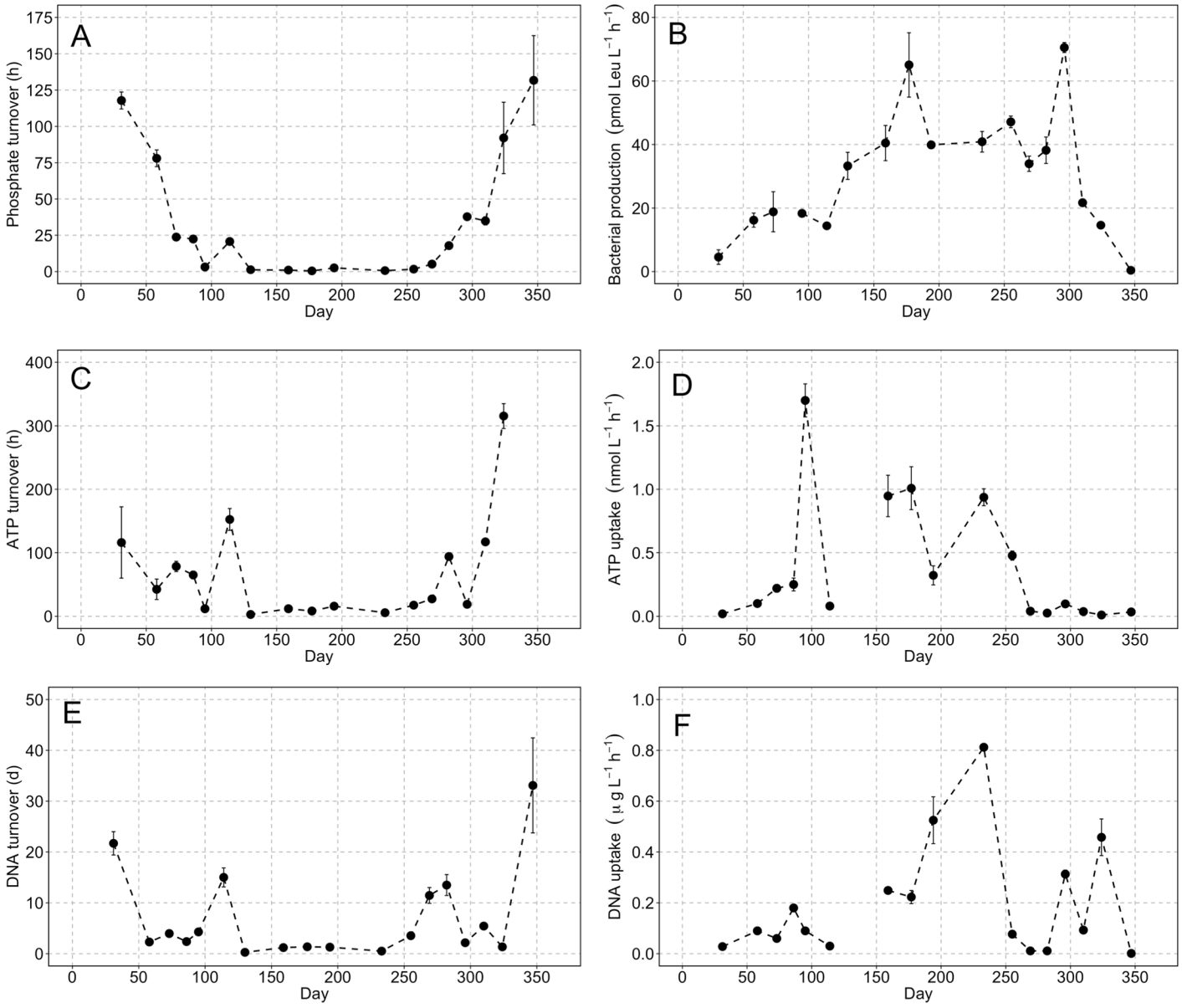

Fig 4. Time-series data of substrate uptake and turnover kinetics. (A) Inorganic phosphate turnover, (B) ATP turnover, (C) ATP uptake, (e) DNA turnover and (F) DNA uptake. Error bars are computed from the LINEST function of the concentration series bioassay data (Tables 1–3). Panel (B) shows community-level leucine incorporation and is taken as an estimate of bacterial production [77]; error bars are from replicate incubations (n = 3). Grey symbols mark the sampling dates when standard environmental parameters were measured and black symbols mark those where the kinetic bioassay experiments were conducted.

https://doi.org/10.1371/journal.pone.0192409.g004

of 3–27 h over the same period (Fig 4C). The high turnover times of ATP and DNA found during summer months correspond to periods of enhanced biological uptake; ATP V_{max} values of 0.32 ± 0.08 to 1.01 ± 0.17 nmol L^{-1} h^{-1} (Fig 4D) and DNA V_{max} values of 0.22 ± 0.03 to 4.47 ± 0.46 ng L^{-1} h^{-1} (Fig 4F) were measured between May and September (Tables 1–3). The highest DNA uptake rate of 4.47 ± 0.46 ng L^{-1} h^{-1} occurred on 9th May corresponding to a salinity minimum of 36.6 PSU (Fig 3B) and the lowest observed DNA turnover of 7.03 ± 0.12 h (Table 3). Leucine incorporation rates were highest during summer months peaking at 70.5 pmol Leu. L^{-1} h^{-1} on the 22nd October.

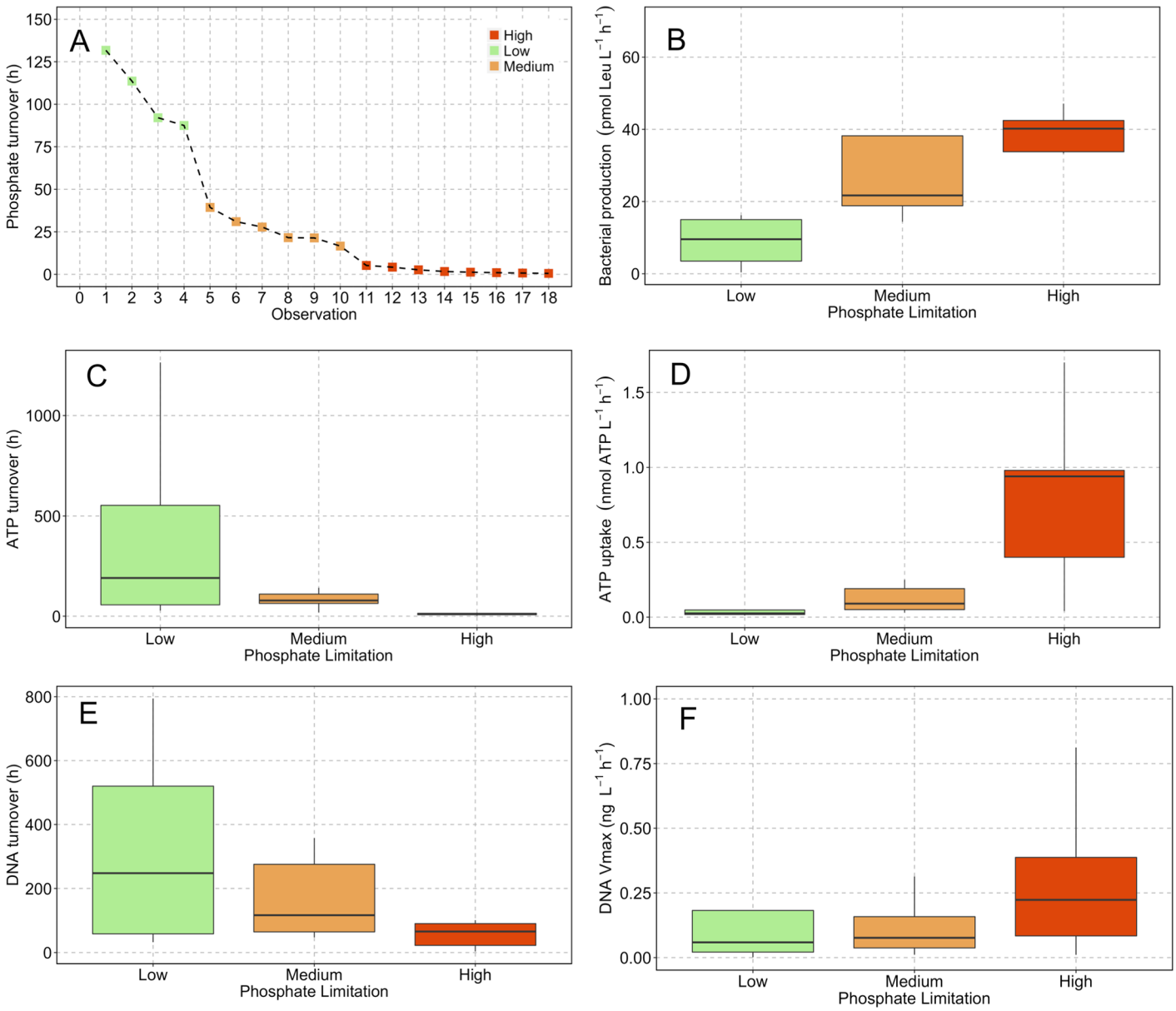

Fig 5. Phosphate limitation categories. Panel (A) shows the empirically derived phosphate limitation categories. Category limits were defined on the basis of successive values increasing by a factor ≥2 and constrained by ensuring that differences between the mean of each category were statistically significant resulting in three categories; high, medium and low phosphate limitation. Panels (B-F) are box and whisker plots of kinetic uptake within these empirically defined categories. Statistically significant differences between the categories are summarized in Table 4.

https://doi.org/10.1371/journal.pone.0192409.g005

Phosphate limitation categories

Phosphate limitation categories were determined by ranking all measures of PO_4^{-3} turnover in descending order (Fig 5A). Categories were subsequently defined on the basis of successive values increasing by a factor ≥2 and constrained by ensuring that differences between the mean of each category were statistically significant. This approach resulted in three categories; high, medium and low phosphate limitation with turnover times of 0.5–5 h, 16–40 h and 90–131 h, respectively (Fig 5A). All permutations of category subset comparisons had

Table 4. Statistical significance of differences in kinetic parameters between phosphate limitation categories. A summary of the results from Welch two sample t-tests comparing the arithmetic means of kinetic parameters between phosphate limitation categories (Fig 5).

Parameter	Phosphate limitation categories		
	High vs. Low	High vs. Medium	Medium vs Low
$^{33}PO_4^{3-}$ (T_0)	<0.001	<0.005	<0.001
AT^{33}P (T_0)	<0.05	n.s.	<0.005
^{33}P-DNA (T_0)	<0.05	n.s.	<0.10
Leucine (V_{max})	<0.025	<0.10	n.s.
AT^{33}P (V_{max})	<0.05	<0.10	<0.025
^{33}P-DNA (V_{max})	n.s. (<0.10)*	n.s.	n.s.

*Results of t-test with DNA outlier removed. See text for further explanation.

https://doi.org/10.1371/journal.pone.0192409.t004

means that were statistically different to each other (Welch two sample t-test) at significance levels $\geq P < 0.005$ (Table 4).

The turnover time of ATP and DNA decreased progressively from low to high phosphate limitation (Fig 5C and 5E). The median decreased from 190>78>9.9 h for ATP turnover and from 248>117>66 h for DNA. Comparison of the arithmetic means (Welch two sample t-test) showed that turnover times between high-low and medium-low phosphate limitation categories are statistically significant (Table 4). Bacterial production rates increased from low to high phosphate limitation (Fig 5B) with median values of 9.6>21.7>40.2 pmol Leu. L^{-1} h^{-1}. The arithmetic means were significantly different in the high-low and high-medium comparison (Table 4). The median values of V_{max} uptake were comparable between low and medium categories: 0.03 cf. 0.09 nmol L^{-1} h^{-1} for ATP and 0.06 cf. 0.08 μg L^{-1} h^{-1} for DNA (Fig 5D and 5E). However, the median V_{max} uptake during high phosphate limitation was notably higher, 0.94 nmol L^{-1} h^{-1} and 0.23 μg L^{-1} h^{-1} for ATP and DNA, respectively. The difference in means for ATP V_{max} was statistically different for each category. The DNA V_{max} dataset was characterized by two extreme values in both the low and high phosphate limitation categories that generate standard errors of 148 and 186%, in part related to the extreme salinity anomaly on 9th May (Fig 3B), for which ATP V_{max} uptake data is not available. These values were identified as outliers by comparing them to the difference between the interquartile range (IQR) and 3rd quartile. Typically if this value is greater than 1.5 a data point can be identified as an outlier in a statistically robust framework. In the case of the DNA V_{max} outliers, they had values of 2.9 and 8.8 for low and high phosphate limitation categories, respectively, and were excluded on this statistical basis resulting in a difference between the arithmetic mean of the high and low phosphate limitation (Table 4).

Partial least squares regression model

The turnover of *d*-eDNA determined from the kinetic bioassay experiments was combined with measured environmental parameters to develop a model that described seasonal *d*-eDNA persistence based on PLS regression analysis (Fig 6). The number of components was selected by examining minimum RMSEP values from 10-fold cross validation and cross-validated r^2 values as measure of goodness of fit to the observed data (S1 File). The model was optimized with two components that described 60% of the observed variance in *d*-eDNA turnover (Fig 6A). Biologically available phosphorous and phosphate turnover, both taken as measures of the degree of phosphate limitation, were the most important variables in the model (Fig 6B).

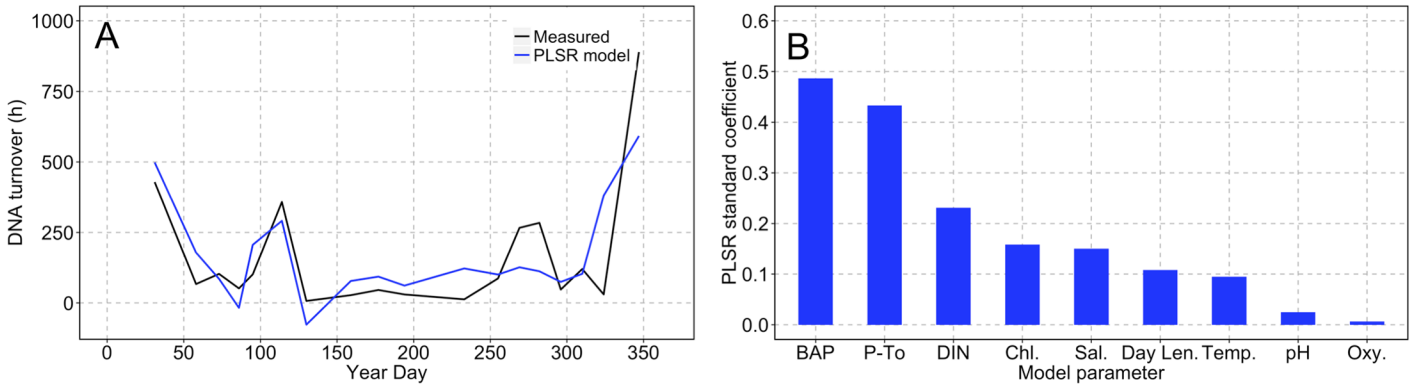

Fig 6. Prediction of dissolved eDNA turnover from environmental parameters. Results from partial latent squares regression (PLSR) model. Panel (A) shows the annual time series of measured *d*-eDNA turnover (black line) and PLSR model output (blue line). Linear regression statistics are slope ± standard error (1.00 ± 0.20), p-value (<0.0005), r^2 (0.60), F-statistic (24.79), degrees of freedom (16), p-value (<0.0005). Panel (B) shows un-signed standardized model coefficients of the environmental parameters in the PLSR model: BAP (biologically available phosphate (k + Sn); Figs 1A and 3C), P-T_0 (phosphate turnover), DIN (dissolved inorganic nitrogen; nitrate + nitrite), Chl. (chlorophyll), Sal. (salinity), Day Len. (day length), Temp. (temperature), pH and Oxy (dissolved oxygen).

https://doi.org/10.1371/journal.pone.0192409.g006

Discussion

The present study demonstrates a strong seasonal component in the turnover of dissolved environmental DNA (*d*-eDNA), ranging from 3 h to > 1 month, in relation to variable environmental conditions. An important consideration of implementing eDNA as a biomonitoring tool concerns the temporal and spatial scales over which the observations can be considered as representative [24,43]. In a dynamic fluid environment, e.g. the coastal ocean, temporal and spatial boundaries are ill defined in comparison to terrestrial ecosystems Consequently the positive detection of a species with the eDNA approach in aquatic settings may represent one of the following: (i) presence of the species at a given site at the time of sampling, (ii) presence of the species at the sampling site from some time previous, or (iii) presence of the species at another location and time; whereby the eDNA signature has been introduced to the sampling site through physical processes such as advection and vertical mixing. The degradation, or turnover time, of eDNA from its point of production is critical in this regard. Although the degradation of eDNA has been recognized as an important constraint on its application [26], and has been addressed in several experimental proof of concept studies [24,42,43], it has not been explicitly considered in natural settings or in the context of seasonal variability. The present findings therefore have important implications when considering the use of eDNA and next generation sequencing approaches to sustained monitoring of biodiversity in marine waters [85], especially when applied to large spatial gradients [20] or time-series observations.

The coastal study site in the Northwest Mediterranean that was the focus of this present study is a phosphorous limited system. Mineral phosphate concentrations, analytically determined as soluble reactive phosphorous (SRP), were < 70 nM and dissolved inorganic nitrogen to phosphate ratios were in excess of Redfield values (median: 28.8); comparable to the Northwest Mediterranean basin as a whole [61,62]. Intuitively phosphate limitation should increase following the spring bloom, however little seasonal variation in SRP concentrations was observed. It has been shown previously that in P-limited environments SRP concentrations over-estimate mineral phosphate concentrations [79], due in part to the acidic conditions of the molybdate reaction that may hydrolyze labile organic phosphorous compounds. Bioavailable phosphate concentrations were estimated from the Rigler bioassay approach and yielded

values that were typically lower than the SRP measurements. Concentration data may obscure variability in the rate a particular nutrient is cycled, especially at low concentrations characterizing nutrient limited systems. In this regard, phosphate turnover is generally considered a more dynamic metric of P-limitation [86]. In the present study both phosphate turnover and bioavailable phosphate concentrations exhibited pronounced seasonal variability characterized by extended periods of minima during summer months. The combination of rapid phosphate cycling (< 5 h), enhanced by elevated temperatures, and low concentrations of bioavailable phosphate (<11 nM) indicate the summer in the coastal Northwest Mediterranean is a period of phosphate limitation.

In the Northwest Mediterranean periods of phosphate limitation ($T_0 < 6$ h) were associated with enhanced uptake and rapid cycling *d*-eDNA. Degrees of phosphate limitation (high, medium, low) were empirically determined for this coastal system based on the seasonal progression of phosphate turnover. The turnover of *d*-eDNA ranged from 3 h during high phosphate limitation to 33 days at low limitation. These results suggest that microbial utilization of *d*-eDNA, as a dissolved organic phosphorous (DOP) substrate [35,50], is an important factor regulating *d*-eDNA persistence in natural marine settings. However, there are numerous factors in the natural environment that could vary to result in the observed seasonal variance of *d*-eDNA persistence. DNA may be denatured directly by abiotic factors such as temperature, UV radiation, pH, dissolved oxygen and salinity [26,39–41,43]. However, some of these considerations are based on extreme environmental gradients (e.g. hypersaline conditions, anoxia, light vs darkness), and may be an inadequate replicate for the seasonally occurring environmental gradients that occur in natural marine systems. For example, in the present study pH ranged from 8.2–8.5, salinity from 36.6–38.2, and dissolved oxygen concentrations from 4.7–6.2 mL L^{-1}, but nevertheless correspond to DNA persistence ranging from several hours to over a month.

In the context of biomonitoring in marine coastal waters, quantifying *d*-eDNA turnover and elucidating the factors responsible for its persistence under natural conditions is necessary. A partial least squares regression (PLSR) model was constructed in an attempt to predict microbial uptake of *d*-eDNA and resulting turnover from seasonal variation in environmental conditions. The PLSR model was capable of explaining 60% of the variance in *d*-eDNA turnover from the observed parameters. Biologically available phosphate concentrations and phosphate turnover, both taken as measures for the degree of phosphate limitation, were the most important factors for predicting *d*-eDNA turnover. Other important biotic factors were chlorophyll and the concentration of dissolved inorganic nitrogen, likely reflecting the onset of phosphate limitation following the spring bloom. The influence of abiotic factors was less important and may be due in part to the weak seasonal gradients of pH, oxygen, UV radiation and salinity occurring at 3 m in the Northwest Mediterranean in comparison to more extreme environmental transitions (e.g. hypersalinity and anoxia). In a natural coastal system, microbial dependence on DOP during periods of phosphate scarcity appears to exert an important control on the seasonal persistence of *d*-eDNA. In the statistical model, approximately 40% of the variance in the observed, microbially mediated, turnover of *d*-eDNA remains unexplained. The PLSR model does not incorporate any information on microbial community structure. The presence of certain bacterial taxa adapted to utilization of DNA as a phosphorus source could explain some of the variance in the model. Notably the largest discrepancy occurs during days 250–300, a period corresponding to the breakdown of summer stratification and shifts in microbial diversity in the Northwest Mediterranean [72]. Incorporating quantification of phylogenetic structure may further constrain the links between microbial nutrient dynamics and *d*-eDNA turnover.

Marine microbes possess a range of strategies for dealing with inorganic P-limitation that either reduces cellular P requirements [86,87] or enzymatically hydrolyses the dissolved organic phosphorous pool [87–91]. Activities of alkaline phosphatase (APA), the enzyme that hydrolyses P-ester bonds in ATP and DNA, are typically enhanced at low SRP concentrations [48,92] and taken as evidence of microbes switching to DOP utilization under P limitation. However, APA enzymatic activities are notably difficult to interpret quantitatively [88] and thus provide little information on rate processes. Direct measurements of ATP uptake using radioactive bioassay approaches are less common: bulk ATP uptake rates measured in P-limited oligotrophic open ocean environments range from 0.22 ± 0.1 nM d^{-1} in the North Atlantic Subtropical gyre [79] to 2.0 ± 0.8 nM d^{-1} in the North Pacific Subtropical gyre [91], although they have been reported as high as 309 nM d^{-1} in extremely P-limited (PO_4^{3-} T_0 = 0.4 h) mesocosm experiments [35]. In the present study, average ATP uptake was 8.9 ± 12 nM d-^{1}, which although is broadly consistent with previous studies covers a much wider range (0.23–40.8 nM d-^{1}) owing to the seasonal variation absent in previous observations.

ATP uptake is commonly used as a model compound to estimate dissolved organic phosphorous (DOP) utilization [89,91,92]. However, the present study is primarily concerned with seasonal variance in the utilization of *d*-eDNA. Earlier work has reported uptake of dissolved DNA in the range of 1.8–8.0 μg L^{-1} h^{-1} [29,35,93]. In the present study dissolved DNA uptake ranges from 0.001–4.5 μg L^{-1} h^{-1}, which is comparable to previous estimates, but as is the case for ATP, covers a broader range indicative of significant seasonal variability. Although ATP and *d*-eDNA turnover follow the same seasonal patterns related to phosphorous limitation, turnover of *d*-eDNA is typically slower. There are very few studies directly comparing turnover of DNA and ATP, but mesocosm enrichment experiments also describe slower turnover rates for DNA [35,50]. The data presented here indicates that ATP and *d*DNA utilization by microbial communities may not be directly comparable, consistent with previous studies that suggest the hydrolysis of DNA involves more complex enzymatic processes than the degradation of monomeric DOP substrates [94].

The similar seasonal patterns observed in ATP and DNA uptake, in addition to leucine incorporation rates, suggest microbes use *d*-eDNA in response to phosphorous limitation. Previous studies have used cell sorting to demonstrate the utilization of ATP as a phosphorous substrate by individual microbial groups including photosynthetic cyanobacteria, heterotrophic bacteria and eukaryotic phytoplankton [87–91]. Considering the hydrolytic enzymes involved in cleaving the P-ester bond, it is reasonable to postulate that the same groups of microbes are responsible for the uptake of *d*-eDNA. Although no direct cell-specific incorporation rates for DNA exist, size-fractionated studies in an experimental mesocosm show DNA uptake to be concentrated in organisms <10 μm [35] and in limnic systems to be concentrated in the bacterial size fraction [29,94]. It is also possible that microbial community structure can influence *d*-eDNA kinetics, if certain phylogenetic groups are differentially limited by phosphate [95,96]. In support of this hypothesis, time-series observations of microbial community structure in the Northwest Mediterranean appear to suggest that seasonal patterns in SAR 11 ecotype abundance are partly linked to phosphorous dynamics [72]. However, in natural systems it is difficult to differentiate whether the distribution of species can drive phosphorous dynamics [97], and by extension *d*-eDNA persistence, or if microbial community structure is an emergent property of environmental filtering [71,72].

The methodology employed in the current study measures biological utilization of the dissolved fraction of the environmental DNA pool. It remains unclear to what extent these results could be generalized for the entire pool of eDNA. There are no studies addressing the seasonal persistence of different size fractions of eDNA in natural marine settings. However, one quantitative experimental study showed that the dissolved fraction (<0.2 μm) accounted for >50%

of total eDNA and 7–25% of Carp eDNA [98], emphasizing the potential significance of the dissolved fraction. Furthermore, fish DNA has been observed at higher concentrations in precipitated versus filtered samples [24], implying both intra- and extracellular sources exist, although methodological differences between filtration and precipitation render such comparisons difficult. Nevertheless, the size distribution of eDNA within the dissolved fraction may also vary [99] and individual components of the dissolved pool can be cycled at different rates [34,100]. The quantitative partitioning of eDNA across different size fractions is likely to depend on the mechanism through which it is introduced into the environment [24]. Urea production from fish, for example, might be better represented in the dissolved fraction than sloughing of epithelial cells or fecal matter. In the latter case, membrane structures might offer some protection to microbial degradation [101,102] that may not be captured with the methodology employed in this study. More research is certainly required on the size distribution of eDNA in natural environments, and in particular how production and decay rates might vary between target organisms and study sites. For example, although the present study highlights the importance of phosphorous dynamics for *d*-eDNA persistence in the natural marine environment, it is important to recognize that P-limitation may be less significant in other environments such as eutrophic or deep-sea ecosystems.

Conclusions

The present study addressed the seasonal variability of dissolved eDNA turnover in marine surface waters of the Northwest Mediterranean. Significant variation in the persistence of *d*-eDNA was linked to microbial utilization of DNA as an organic phosphorous substrate under conditions of seasonal phosphate limitation. The future application of eDNA as a long-term biomonitoring tool for biodiversity and conservation should take seasonal variability into account, particularly in phosphate-limited water bodies. It is hypothesized that seasonal variability in eDNA turnover exists in other aquatic settings, although it may be driven by factors other than phosphorous limitation. Furthermore, it is suggested that the seasonal persistence of eDNA is decoupled across naturally occurring size fractions, resulting in differential artifacts depending on the target organism(s) and the environment in which they occur. In order to correctly understand the spatial and temporal scales of e-DNA species detection, future studies should aim to constrain the natural variability in DNA degradation kinetics for the system in question.

Supporting information

S1 File. PLSR model validation. Description of the model assumptions and cross validation technique used in PLSR development.
(PDF)

S2 File. Source code. Archive of R source code used in the manuscript.
(PDF)

S3 File. Compressed raw data files. Files containing all of the raw data used in the manuscript.
(ZIP)

Acknowledgments

I thank LEFE-CYBER for financial support of POPPY-MED. I also acknowledge Eric Maria, Cyrielle Tricoire, and Louise Oriol for technical support in collecting samples to contribute towards the SOMLIT coastal observation program and Maria Nielsdóttir for proof reading.

Author Contributions

Conceptualization: Ian Salter.

Funding acquisition: Ian Salter.

Investigation: Ian Salter.

Methodology: Ian Salter.

Project administration: Ian Salter.

Validation: Ian Salter.

Writing – original draft: Ian Salter.

Writing – review & editing: Ian Salter.

References

1. Magurran AE. Measuring Biological Diversity. Wiley-Blackwell; 2004.
2. Ficetola GF, Miaud C, Pompanon F, Taberlet P. Species detection using environmental DNA from water samples. Biol Lett. 2008; 4: 423–425. https://doi.org/10.1098/rsbl.2008.0118 PMID: 18400683
3. Curtin R, Prellezo R. Understanding marine ecosystem based management: A literature review. Mar Policy. 2010; 34: 821–830. https://doi.org/10.1016/j.marpol.2010.01.003
4. Bohmann K, Evans A, Gilbert MTP, Carvalho GR, Creer S, Knapp M, et al. Environmental DNA for wildlife biology and biodiversity monitoring. Trends Ecol Evol. 2014; 29: 358–367. https://doi.org/10.1016/j.tree.2014.04.003 PMID: 24821515
5. Aylagas E, Borja Á, RodrÍguez-Ezpeleta N. Environmental status assessment using DNA metabarcoding: Towards a genetics based marine biotic index (gAMBI). PLoS One. 2014; 9. https://doi.org/10.1371/journal.pone.0090529 PMID: 24603433
6. Danovaro R, Carugati L, Berzano M, Cahill AE, Carvalho S, Chenuil A, et al. Implementing and Innovating Marine Monitoring Approaches for Assessing Marine Environmental Status. Front Mar Sci. 2016; 3: 1–25. https://doi.org/10.3389/fmars.2016.00213
7. Pace NR. A Molecular View of Microbial Diversity and the Biosphere. Science (80-). 1997; 276: 734–740. https://doi.org/10.1126/science.276.5313.734
8. Logares R, Audic S, Bass D, Bittner L, Boutte C, Christen R, et al. Patterns of Rare and Abundant Marine Microbial Eukaryotes. Curr Biol. 2014; 24: 813–821. https://doi.org/10.1016/j.cub.2014.02.050 PMID: 24704080
9. Taberlet P, Coissac E, Pompanon F, Brochmann C, Willerslev E. Towards next-generation biodiversity assessment using DNA metabarcoding. Mol Ecol. 2012; 21: 2045–2050. https://doi.org/10.1111/j.1365-294X.2012.05470.x PMID: 22486824
10. Thomsen PF, Kielgast J, Iversen LL, Wiuf C, Rasmussen M, Gilbert MTP, et al. Monitoring endangered freshwater biodiversity using environmental DNA. Mol Ecol. 2012; 21: 2565–2573. https://doi.org/10.1111/j.1365-294X.2011.05418.x PMID: 22151771
11. Goodwin KD, Thompson LR, Duarte B, Kahlke T, Thompson AR, Marques JC, et al. DNA Sequencing as a Tool to Monitor Marine Ecological Status. Front Mar Sci. 2017; 4: 1–14. https://doi.org/10.3389/fmars.2017.00107
12. Goldberg CS, Sepulveda A, Ray A, Baumgardt J, Waits LP. Environmental DNA as a new method for early detection of New Zealand mudsnails (*Potamopyrgus antipodarum*). Freshw Sci. 2013; 32: 792–800. https://doi.org/10.1899/13-046.1
13. Piaggio AJ, Engeman RM, Hopken MW, Humphrey JS, Keacher KL, Bruce WE, et al. Detecting an elusive invasive species: A diagnostic PCR to detect Burmese python in Florida waters and an assessment of persistence of environmental DNA. Mol Ecol Resour. 2014; 14. https://doi.org/10.1111/1755-0998.12180 PMID: 24119154
14. Valentini A, Taberlet P, Miaud C, Civade R, Herder J, Thomsen PF, et al. Next-generation monitoring of aquatic biodiversity using environmental DNA metabarcoding. Mol Ecol. 2016; https://doi.org/10.1111/mec.13428 PMID: 26479867
15. Thomsen PF, Kielgast J, Iversen LL, Müller PR, Rasmussen M, Willerslev E. Detection of a Diverse Marine Fish Fauna Using Environmental DNA from Seawater Samples. PLoS One. 2012; 7: 1–9. https://doi.org/10.1371/journal.pone.0041732 PMID: 22952584

16. Takahara T, Minamoto T, Yamanaka H, Doi H, Kawabata Z. Estimation of fish biomass using environmental DNA. PLoS One. 2012; 7: 1–8. https://doi.org/10.1371/journal.pone.0035868 PMID: 22563411

17. Kelly RP, Port JA, Yamahara KM, Crowder LB. Using environmental DNA to census marine fishes in a large mesocosm. PLoS One. 2014; 9: 1–11. https://doi.org/10.1371/journal.pone.0086175 PMID: 24454960

18. Lacoursière-Roussel A, Rosabal M, Bernatchez L. Estimating fish abundance and biomass from eDNA concentrations: variability among capture methods and environmental conditions. Mol Ecol Resour. 2016; 16: 1401–1414. https://doi.org/10.1111/1755-0998.12522 PMID: 26946353

19. Thomsen PF, Møller PR, Sigsgaard EE, Knudsen SW, Jørgensen OA, Willerslev E. Environmental DNA from seawater samples correlate with trawl catches of subarctic, deepwater fishes. PLoS One. 2016; 11: 1–22. https://doi.org/10.1371/journal.pone.0165252 PMID: 27851757

20. Andruszkiewicz EA, Starks HA, Chavez FP, Sassoubre LM, Block BA, Boehm AB. Biomonitoring of marine vertebrates in Monterey Bay using eDNA metabarcoding. PLoS One. 2017; 12: 1–20. https://doi.org/10.1371/journal.pone.0176343 PMID: 28441466

21. Foote AD, Thomsen PF, Sveegaard S, Wahlberg M, Kielgast J, Kyhn LA, et al. Investigating the Potential Use of Environmental DNA (eDNA) for Genetic Monitoring of Marine Mammals. PLoS One. 2012; 7: 1–6. https://doi.org/10.1371/journal.pone.0041781 PMID: 22952587

22. Sigsgaard EE, Nielsen IB, Bach SS, Lorenzen ED, Robinson DP, Knudsen SW, et al. Population characteristics of a large whale shark aggregation inferred from seawater environmental DNA. Nat Ecol Evol. 2016; 1: 1–4. https://doi.org/10.1038/s41559-016-0004 PMID: 28812572

23. Nielsen KM, Johnsen PJ, Bensasson D, Daffonchio D. Thematic Issue on Horizontal Gene Transfer Review Release and persistence of extracellular DNA in the environment. Environ Biosaf Res. 2007; 6: 37–53.

24. Sassoubre LM, Yamahara KM, Gardner LD, Block BA, Bohem AB. Quantification of environmental DNA (eDNA) Shedding and Decay Rates for Three Marine Fish. Environ Sci Technol. 2016; 50: 10456–10464. https://doi.org/10.1021/acs.est.6b03114 PMID: 27580258

25. Dejean T, Valentini A, Duparc A, Pellier-Cuit S, Pompanon F, Taberlet P, et al. Persistence of environmental DNA in freshwater ecosystems. PLoS One. 2011; https://doi.org/10.1371/journal.pone.0023398 PMID: 21858099

26. Barnes MA, Turner CR, Jerde CL, Renshaw MA, Chadderton LW, Lodge DM. Environmental Conditions Influence eDNA Persistence in Aquatic Systems. Environ Sci Technol. 2014; 48: 1819–1827. https://doi.org/10.1021/es404734p PMID: 24422450

27. Albano M, Hahn J, Dubnau D. Expression of Competence Genes in Bacillus subtilis. J Bacteriol. 1987; 169: 3110–3117. PMID: 3110135

28. Deflaun MF, Paul JH, Jeffrey WH. Distribution and molecular weight of dissolved DNA in subtropical estuarine and oceanic environments. Mar Ecol Prog Ser. 1987; 38: 65–73. https://doi.org/10.3354/meps038065

29. Paul JH, Jeffrey WH, Deflaun MF. Dynamics of Extracellular DNA in the Marine Environment. Appl Environ Microbiol. 1987; 53: 170–179. PMID: 3827244

30. Paul JH, Deflaun MF, Jeffrey WH. Mechanisms of DNA Utilization by Estuarine Microbial Populations. Appl Environ Microbiol. 1988; 54: 1682–1688. PMID: 16347679

31. Paul JH, Deflaun MF, Jeffrey WH, David AW. Seasonal and Diel Variability in Dissolved DNA and in Microbial Biomass and Activity in a Subtropical Estuary. Appl Environ Microbiol. 1988; 54: 718–727. PMID: 16347583

32. Paul JH, Jeffrey WH, David AW, Deflaun MF, Cazares LH. Turnover of Extracellular DNA in Eutrophic and Oligotrophic Freshwater Environments of Southwest Florida. Appl Environ Microbiol. 1989; 55: 1823–1828. PMID: 16347976

33. Jørgensen NOG, Jacobsen CS. Bacterial uptake and utilization of dissolved DNA. Aquat Microb Ecol. 1996; 11: 263–270. https://doi.org/10.3354/ame011263

34. Brum J. Concentration, production and turnover of viruses and dissolved DNA pools at stn ALOHA, North Pacific Subtropical Gyre. Aquat Microb Ecol. 2005; 41: 103–113. https://doi.org/10.3354/ame041103

35. Løvdal T, Tanaka T, Thingstad TF. Algal-bacterial competition for phosphorus from dissolved DNA, ATP, and orthophosphate in a mesocosm experiment. Limnol Oceanogr. 2007; 52: 1407–1419. https://doi.org/10.4319/lo.2007.52.4.1407

36. Ammerman JW, Azam F. Bacterial 5'-Nucleotidase in Aquatic Ecosystems: A Novel Mechanism of Phosphorus Regeneration. Science (80-). 1985; 227: 1338–1340. https://doi.org/10.1126/science.227.4692.1338 PMID: 17793769

37. Chróst RJ. Microbial ectoenzymes in aquatic environments. In: Overbeck J, Chróst RJ, editors. Aquatic microbial ecology: Biochemical and molecular approaches. New York: Springer-Verlag; 1990. pp. 47–78. https://doi.org/10.1007/978-1-4612-3382-4

38. Ammerman JW, Azam F. Bacterial 5'-nucleotidase activity in estuarine and coastal marine waters: Characterization of enzyme activity. Limnol Oceanogr. 1991; 36: 1427–1436. https://doi.org/10.4319/lo.1991.36.7.1427

39. Ravanat J, Douki T, Cadet J. Direct and indirect effects of UV radiation on DNA and its components. J Photochem Photobiol B Biol. 2001; 63: 88–102.

40. Green HC, Shanks OC, Sivaganesan M, Haugland RA, Field KG. Differential decay of human faecal Bacteroides in marine and freshwater. Environ Microbiol. 2011; 13: 3235–3249. https://doi.org/10.1111/j.1462-2920.2011.02549.x PMID: 21883797

41. Pilliod DS, Goldberg CS, Arkle RS, Waits LP. Factors influencing detection of eDNA from a stream-dwelling amphibian. Mol Ecol Resour. 2014; 14. https://doi.org/10.1111/1755-0998.12159 PMID: 24034561

42. Strickler KM, Fremier AK, Goldberg CS. Quantifying effects of UV-B, temperature, and pH on eDNA degradation in aquatic microcosms. Biol Conserv. 2015; 183: 85–92. https://doi.org/10.1016/j.biocon.2014.11.038

43. Eichmiller JJ, Best SE, Sorensen PW. Effects of Temperature and Trophic State on Degradation of Environmental DNA in Lake Water. Environ Sci Technol. 2016; 50: 1859–1867. https://doi.org/10.1021/acs.est.5b05672 PMID: 26771292

44. Borin S, Crotti E, Mapelli F, Tamagnini I, Corselli C, Daffonchio D. DNA is preserved and maintains transforming potential after contact with brines of the deep anoxic hypersaline lakes of the Eastern Mediterranean Sea. Saline Systems. 2008; 4.

45. Hofreiter M, Serre D, Poinar H. N., Kuch M, Pääbo S. Ancient DNA. Nat Rev Genet. 2001; 2: 353–359. https://doi.org/10.1038/35072071 PMID: 11331901

46. Ammerman JW, Azam F. Bacterial S-nucleotidase activity in Role in phosphorus regeneration. Limnol Oceanogr. 1991; 36: 1437–1447. https://doi.org/10.4319/lo.1991.36.7.1437

47. Thingstad TF, Skjoldal EF, Bohne RA. Phosphorus cycling and algal-bacterial competition in Sandsfjord, western Norway. Mar Ecol Prog Ser. 1993; 99: 239–259. https://doi.org/10.3354/meps099239

48. Mather RL, Reynolds SE, Wolff GA, Williams RG, Torres-Valdes S, Woodward EMS, et al. Phosphorus cycling in the North and South Atlantic Ocean subtropical gyres. Nat Geosci. 2008; 1: 439–443. https://doi.org/10.1038/ngeo232

49. Clark LL, Ingall ED, Benner R. Marine Organic Phosphorous Cycling: Novel insights from nuclear magnetic resonance. Am J Sci. 1999; 2999: 724–737.

50. Løvdal T, Eichner C, Grossart H-P, Carbonnel V, Chou L, Martin-Jézéquel V, et al. Competition for inorganic and organic forms of nitrogen and phosphorous between phytoplankton and bacteria during an Emiliania huxleyi spring bloom. Biogeosciences. 2008; 5: 371–383. https://doi.org/10.5194/bg-5-371-2008

51. Coll M, Piroddi C, Steenbeek J, Kaschner K, Lasram FBR, Aguzzi J, et al. The biodiversity of the Mediterranean Sea: Estimates, patterns, and threats. PLoS ONE. 2010. https://doi.org/10.1371/journal.pone.0011842 PMID: 20689844

52. Danovaro R, Dinet A, Duineveld G, Tselepides A. Benthic response to particulate fluxes in different trophic environments: a comparison between the Gulf of Lions–Catalan Sea (western-Mediterranean) and the Cretan Sea (eastern-Mediterranean). Prog Oceanogr. 1999; 44: 287–312. https://doi.org/10.1016/S0079-6611(99)00030-0

53. Coll M, Piroddi C, Albouy C, Ben Rais Lasram F, Cheung WWL, Christensen V, et al. The Mediterranean Sea under siege: Spatial overlap between marine biodiversity, cumulative threats and marine reserves. Glob Ecol Biogeogr. 2012; 21: 465–480. https://doi.org/10.1111/j.1466-8238.2011.00697.x

54. Sala E, Kizilkaya Z, Yildirim D, Ballesteros E. Alien marine fishes deplete algal biomass in the Eastern Mediterranean. PLoS One. 2011; 6. https://doi.org/10.1371/journal.pone.0017356 PMID: 21364943

55. Zenetos A, Gofas S, Morri C, Rosso A, Violanti D, García Raso JE, et al. Alien species in the Mediterranean Sea by 2012. A contribution to the application of European Union's Marine Strategy Framework Directive (MSFD). Part 2. Introduction trends and pathways. Medit Mar Sci. 2012; 13: 328–352. https://doi.org/10.12681/mms.327

56. Bearzi G, Holcer D, Di Sciara GN. The role of historical dolphin takes and habitat degradation in shaping the present status of northern Adriatic cetaceans. Aquat Conserv Mar Freshw Ecosyst. 2004; 14: 363–379. https://doi.org/10.1002/aqc.626

57. Sala E. The past and present topology and structure of mediterranean subtidal rocky-shore food webs. Ecosystems. 2004; 7: 333–340. https://doi.org/10.1007/s10021-003-0241-x

58. Ferretti F, Myers RA, Serena F, Lotze HK. Loss of Large Predatory Sharks from the Mediterranean Sea. Conserv Biol. 2008; 22: 952–964. https://doi.org/10.1111/j.1523-1739.2008.00938.x PMID: 18544092

59. Sala E, Ballesteros E, Dendrinos P, Di Franco A, Ferretti F, Foley D, et al. The structure of mediterranean rocky reef ecosystems across environmental and human gradients, and conservation implications. PLoS One. 2012; 7. https://doi.org/10.1371/journal.pone.0032742 PMID: 22393445

60. Ignatiades L. Scaling the trophic status of the Aegean Sea, eastern Mediterranean. J Sea Res. 2005; 54: 51–57. https://doi.org/10.1016/j.seares.2005.02.010

61. Pujo-Pay M, Conan P, Oriol L, Cornet-Barthaux V, Falco C, Ghiglione JF, et al. Integrated survey of elemental stoichiometry (C, N, P) from the western to eastern Mediterranean Sea. Biogeosciences. 2011; 8: 883–889. https://doi.org/10.5194/bg-8-883-2011

62. Lazzari P, Solidoro C, Salon S, Bolzon G. Spatial variability of phosphate and nitrate in the Mediterranean Sea: A modeling approach. Deep Sea Res Part I Oceanogr Res Pap. 2016; 108: 39–52. https://doi.org/10.1016/j.dsr.2015.12.006

63. Moutin T, Raimbault P. Primary production, carbon export and nutrients availability in western and eastern Mediterranean Sea in early summer 1996 (MINOS cruise). J Mar Syst. 2002; 33–34: 273–288. https://doi.org/10.1016/S0924-7963(02)00062-3

64. López-Sandoval DC, Fernández A, Marañón E. Dissolved and particulate primary production along a longitudinal gradient in the Mediterranean Sea. Biogeosciences. 2011; 8: 815–825. https://doi.org/10.5194/bg-8-815-2011

65. Krom MD, Kress N, Brenner S, Gordon LI. Phosphorous limitation of primary productivity in the eastern Mediterranean Sea. Limnol Oceanogr. 1991; 36: 424–432. https://doi.org/10.4319/lo.1991.36.3.0424

66. Krom MD, Thingstad TF, Brenner S, Carbo P, Drakopoulos P, Fileman TW, et al. Summary and overview of the CYCLOPS P addition Lagrangian experiment in the Eastern Mediterranean. Deep Sea Res Part II Top Stud Oceanogr. 2005; 52: 3090–3108. https://doi.org/10.1016/j.dsr2.2005.08.018

67. Thingstad TF, Krom MD, Mantoura RFC, Flaten GAF, Groom S, Herut B, et al. Nature of Phosphorus Limitation in the Ultraoligotrophic Eastern Mediterranean. Science (80-). 2005; 309: 1068–1071. https://doi.org/10.1126/science.1112632 PMID: 16099984

68. Van Wambeke F, Christaki U, Giannakourou A, Moutin T, Souvemerzoglou K. Longitudinal and vertical trends of bacterial limitation by phosphorus and carbon in the Mediterranean Sea. Microb Ecol. 2002; 43: 119–133. https://doi.org/10.1007/s00248-001-0038-4 PMID: 11984634

69. Sebastián M, Pitta P, González JM, Thingstad TF, Gasol JM. Bacterioplankton groups involved in the uptake of phosphate and dissolved organic phosphorus in a mesocosm experiment with P-starved Mediterranean waters. Environ Microbiol. 2012; 14: 2334–2347. https://doi.org/10.1111/j.1462-2920.2012.02772.x PMID: 22564346

70. Obernosterer I, Lami R, Larcher M, Batailler N, Catala P, Lebaron P. Linkage between bacterial carbon processing and the structure of the active bacterial community at a coastal site in the NW Mediterranean Sea. Microb Ecol. 2010; 59: 428–435. https://doi.org/10.1007/s00248-009-9588-7 PMID: 19789909

71. Galand PE, Salter I, Kalenitchenko D. Ecosystem productivity is associated with bacterial phylogenetic distance in surface marine waters. Mol Ecol. 2015; https://doi.org/10.1111/mec.13347 PMID: 26289961

72. Salter I, Galand PE, Fagervold SK, Lebaron P, Obernosterer I, Oliver MJ, et al. Seasonal dynamics of active SAR11 ecotypes in the oligotrophic Northwest Mediterranean Sea. ISME J. 2015; 9: 347–360. https://doi.org/10.1038/ismej.2014.129 PMID: 25238399

73. Yentsch CM, Menzel DW. A Method for the determination of phytoplankton chlorophyll and phaeophytin by fluorescence. Deep Sea Res Oceanogr Abstr. 1963; 10: 221–231. https://doi.org/10.1016/0011-7471(63)90358-9

74. Strickland JD., Parsons TR. A prectical handbook of seawater analsis. Ottawa: Fisheries Research Board of Canada; 1972.

75. Treguer P, Le Corre P. Manuel d'analyse des sels nutritifs dans l'eau de mer. Utilisation de l'autoanalyseur II, Technicon. Brest: Université de Bretagne Occidentale; 1974.

76. Aminot A, Kérouel R. Dosage automatique des nutriments dans les eaux marines: méthodes en flux continu. In: Ifremer, editor. méthodes d'analyse en milieu marin. 2007. p. 188.

77. Smith DC, Azam F. A simple, economical method for measuring bacterial protein synthesis rates in seawater using 3H-leucine. Mar Microb Food Webs. 1992; 6: 107–114.

78. Rigler FH. Radiobiological analysis of inorganic phosphorus in lakewater. Verhandlungen Int für theorestische und angwandte Limnol. 1966; 465–470.

79. Zubkov M V., Mary I, Woodward EMS, Warwick PE, Fuchs BM, Scanlan DJ, et al. Microbial control of phosphate in the nutrient-depleted North Atlantic subtropical gyre. Environ Microbiol. 2007; 9: 2079–2089. https://doi.org/10.1111/j.1462-2920.2007.01324.x PMID: 17635551

80. Hodgson CP, Fisk RZ. Hybridization probe size control: Optimized oligolabelling. Nucleic Acids Res. 1987; 15: 6295. https://doi.org/10.1093/nar/15.15.6295 PMID: 3627988

81. Sambrook J, Russell DW. Molecular cloning: A laboratory journal. 3rd ed. New York: Cold Spring Harbour Laboratory Press; 2001.

82. Talarmin A, Van Wambeke F, Duhamel S, Catala P, Moutin T, Lebaron P. Improved methodology to measure taxon-specific phosphate uptake in live and unfiltered samples. Limnol Oceanogr Methods. 2011; 9: 443–453. https://doi.org/10.4319/lom.2011.9.443

83. Wold S, Sjostrom M, Eriksson L. PLS-regression: a basic tool of chemometrics. Chemom Intell Lab Syst. 2001; 58: 109–130. https://doi.org/10.1016/S0169-7439(01)00155-1

84. Sanchez G. Package "plsdepot" Title Partial Least Squares (PLS) Data Analysis Methods. 2016.

85. Aylagas E, Borja Á, Irigoien X, Rodríguez-Ezpeleta N. Benchmarking DNA Metabarcoding for Biodiversity-Based Monitoring and Assessment. Front Mar Sci. 2016; 3: 1–12. https://doi.org/10.3389/fmars.2016.00096

86. Van Mooy BAS, Fredricks HF, Pedler BE, Dyhrman ST, Karl DM, Koblížek M, et al. Phytoplankton in the ocean use non-phosphorus lipids in response to phosphorus scarcity. Nature. 2009; 458: 69–72. https://doi.org/10.1038/nature07659 PMID: 19182781

87. Popendorf KJ, Duhamel S. Variable phosphorus uptake rates and allocation across microbial groups in the oligotrophic Gulf of Mexico. Environ Microbiol. 2015; 17: 3992–4006. https://doi.org/10.1111/1462-2920.12932 PMID: 26033372

88. Casey JR, Lomas MW, Michelou VK, Dyhrman ST, Orchard ED, Ammerman JW, et al. Phytoplankton taxon-specific orthophosphate (Pi) and ATP utilization in the western subtropical North Atlantic. Aquat Microb Ecol. 2010; 58: 31–44. https://doi.org/10.3354/ame01348

89. Orchard ED, Ammerman JW, Lomas MW, Dyhrman ST. Dissolved inorganic and organic phosphorus uptake in Trichodesmium and the microbial community: The importance of phosphorus ester in the Sargasso Sea. Limnol Oceanogr. 2010; 55: 1390–1399. https://doi.org/10.4319/lo.2010.55.3.1390

90. Michelou VK, Lomas MW, Kirchman DL. Phosphate and adenosine-5'-triphosphate uptake by cyanobacteria and heterotrophic bacteria in the Sargasso Sea. Limnol Oceanogr. 2011; 56: 323–332. https://doi.org/10.4319/lo.2011.56.1.0323

91. Björkman K, Duhamel S, Karl DM. Microbial group specific uptake kinetics of inorganic phosphate and adenosine-5'-triphosphate (ATP) in the North Pacific Subtropical Gyre. Front Microbiol. 2012; 3: 1–17.

92. Duhamel S, Dyhrman ST, Karl DM. Alkaline phosphatase activity and regulation in the North Pacific Subtropical Gyre. Limnol Oceanogr. 2010; 55: 1414–1425. https://doi.org/10.4319/lo.2010.55.3.1414

93. Siuda W, Chróst RJ, Güde H. Distribution and origin of dissolved DNA in lakes of different trophic states. Aquat Microb Ecol. 1998; 15: 89–96. https://doi.org/10.3354/ame015089

94. Siuda W, Güde H. Evaluation of dissolved DNA and nucleotides as potential sources of phosphorus for plankton organisms in Lake Constance. Arch Hydrobiol Spec Issues Adv Limnol. 1996; 48: 155–162.

95. Fu FX, Zhang Y, Bell PRF, Hutchins DA. Phosphate uptake and growth kinetics of Trichodesmium (Cyanobacteria) isolates from the North Atlantic Ocean and the Great Barrier Reef, Australia. J Phycol. 2005; 41. https://doi.org/10.1111/j.1529-8817.2005.04063.x

96. Fu F-X, Zhang Y, Feng Y, Hutchins DA. Phosphate and ATP uptake and growth kinetics in axenic cultures of the cyanobacterium Synechococcus CCMP 1334 Phosphate and ATP uptake and growth kinetics in axenic cultures of the cyanobacterium Synechococcus CCMP 1334. Eur J Phycol. 2006; 41: 15–28.

97. Lomas MW, Bonachela JA, Levin SA, Martiny AC. Impact of ocean phytoplankton diversity on phosphate uptake. Proc Natl Acad Sci. 2014; 111: 17540–17545. https://doi.org/10.1073/pnas.1420760111 PMID: 25422472

98. Turner CR, Barnes MA, Xu CCY, Jones SE, Jerde CL, Lodge DM. Particle size distribution and optimal capture of aqueous macrobial eDNA. Methods Ecol Evol. 2014; https://doi.org/10.1111/2041-210X.12206

99. Jiang SC, Paul JH. Viral contribution to dissolved DNA in the marine environment as determined by differential centrifugation and kingdom probing. Appl Environ Microbiol. 1995; 61: 317–325. PMID: 16534913

100. Siuda W, Chróst RJ. Concentration and susceptibility of dissolved DNA for enzyme degradation in lake water—Some methodological remarks. Aquat Microb Ecol. 2000; 21: 195–201. https://doi.org/10.3354/ame021195

101. Walters SP, Yamahara KM, Boehm AB. Persistence of nucleic acid markers of health-relevant organisms in seawater microcosms: Implications for their use in assessing risk in recreational waters. Water Res. 2009; 43: 4929–4939. https://doi.org/10.1016/j.watres.2009.05.047 PMID: 19616273

102. Boere AC, Sinninghe Damsté JS, Rijpstra WIC, Volkman JK, Coolen MJL. Source-specific variability in post-depositional DNA preservation with potential implications for DNA based paleoecological records. Org Geochem. 2011; 42: 1216–1225. https://doi.org/10.1016/j.orggeochem.2011.08.005